



Westinghouse
Electric Corporation

Energy Systems

Box 355
Pittsburgh Pennsylvania 15230-0355

DCP/NRC1021
NSD-NRC-97-5307
Docket No.: 52-003

September 23, 1997

Document Control Desk
U.S. Nuclear Regulatory Commission
Washington, DC 20555

ATTENTION: T. R. QUAY

SUBJECT: AP600 RESPONSE TO REQUEST FOR ADDITIONAL INFORMATION

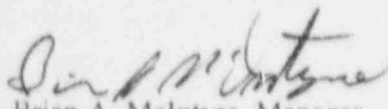
- Reference:
1. WCAP-14967, "Assessment of Effects of WGOthic Solver Upgrade from Version 1.2 to 4.1," September 1997.
 2. Westinghouse Letter DCP/NRC1019, dated September 8, 1997.

Dear Mr. Quay:

Enclosed is the Westinghouse response to the NRC request for additional information, RAI 480.1023, related to the WGOthic solver upgrade from version 1.2 to 4.1. Reference 1 contains additional information on this topic, and was transmitted to NRC via Reference 2.

This response closes, from the Westinghouse perspective, this item. The NRC should review this response and inform Westinghouse of the status to be designated in the "NRC Status" column of the OITS.

Please contact Bruce Rarig on (412) 374-4358 if you have any questions concerning this submittal.


 Brian A. McIntyre, Manager
 Advanced Plant Safety and Licensing

jml

Enclosure

cc: D. C. Scaletti, NRC (w/ Enclosure)
 N. J. Liparulo, Westinghouse (w/o Enclosure)

E00411

3300a wpf

9709250222 970923
 PDR ADOCK 05200003
 A PDR





OITS: 5461
RAI: 480.1023

SECTION 12, "CLIME NODING STUDY," OF WCAP-14407, "WGOthic APPLICATION REPORT"

The applicant needs to provide an evaluation of the differences between WGOthic Versions 1.2 and 4.1 on the previous calculations presented in the "WGOthic Code Description and Validation" report, WCAP-14382. This evaluation should present a technical justification why these existing calculations remain valid, and consider the "ccvel" subroutine and the changes to the annulus inertia lengths. Those calculations deemed most likely to be impacted by the change from Version 1.2 to Version 4.1 should be rerun (at a minimum, Tests 214.1A, 214.1B, 216.1B, 219.1A, 219.1B, 219.1C, and 222.4B) and provide comparison plots of pressure, passive containment cooling system (PCS) air and film temperature, heat flux, and heat removal rate.

Response:

An assessment of the differences between WGOthic solver versions 1.2 and 4.1 is provided in Reference 480.1023-1. As described in Section 3 of Reference 480.1023-1, the conclusions of the WGOthic code validation documented in Reference 480.1023-2 remain valid for WGOthic version 4.1.

Reference 480.1023-1 includes plots of transient vessel pressure, as well as plots of other data used in the assessment. The following additional plots requested by this RAI are provided herein:

- transient rate of vessel heat removal both into and out of the shell
- transient PCS film exit and air outlet temperatures
- circumferentially averaged heat flux as a function of height

Differences in code version results shown in this RAI response do not alter the conclusions of Reference 480.1023-1.

Some comments that are applicable across the spectrum of tests are presented below. The comparison plots show WGOthic version 4.1 results as a solid line and version 1.2 results as a dashed line. A description of the LST WGOthic lumped parameter model referred to in the response is given in WCAP-14382 (Ref. 480.1023-2), Section 6.0. The liquid film exit temperature is given for each LST WGOthic simulation described below. There are four wet



climes from which the film exits. Since the film exit temperatures for each of these climes are approximately equal, the result for only one clime is shown for simplicity.

LST 219.1

Test 219.1 was performed at a constant steam flow and with forced air cooling. The vessel pressure came to steady state under constant steam flow and a dry vessel (219.1A). Helium was then injected and the vessel pressure allowed to come to steady state again (219.1B). Then the water was turned on and the vessel pressure steadied to a third level (219.1C). The steady state water coverage for test 219.1C is described in Reference 480.1023-1, Appendix B.

The predicted heat rate into and out of the containment shell are shown in Figures 480.1023-1 and 480.1023-2, respectively. The heat rate for version 1.2 is higher than version 4.1 when the water is first put onto the vessel due to the method used to determine clime dry out. The corrected clime dryout model used in version 4.1 results in a lower predicted heat rate. Clime dryout occurs from 34,400 seconds - 35,400 seconds, and at 35,800 seconds, during the initial water application. After the initial spike, a quasi-steady heat removal rate equivalent to the net steam energy delivery rate (which remained essentially constant through the transient) is reached, at which time the vessel pressure is significantly reduced due to the addition of water cooling.

The predicted transient PCS liquid film exit temperature is shown in Figure 480.1023-3. When the clime is dry (from 0 - 34,400 seconds) the plot shows the dry surface temperature. After water is put onto the vessel, the plot shows the external liquid film exit temperature. The predicted transient PCS air outlet temperature is shown in Figure 480.1023-4.

The predicted circumferentially averaged heat flux is shown as a function of height for test 219.1 steady state phases A, B, and C in Figures 480.1023-5 through 480.1023-7, respectively.

LST 214.1

The initial phase of test 214.1 is natural convection (214.1A); the second phase is forced convection (214.1B), with the fan being turned on at 9260 seconds. The water coverage for test 214.1 is described in Reference 480.1023-1, Appendix B. The steam flow rate is held essentially constant throughout the test.

The predicted heat rates into and out of the PCS shell are shown in Figures 480.1023-8 and 480.1023-9, respectively. The spikes in heat rates at ~3000 seconds and ~10,000 seconds are





an effect of an instantaneous change in the code water coverage fraction input value described in Reference 480.1023-1, Appendix B.

The predicted film outlet temperatures are shown in Figure 480.1023-10. The predicted film temperature is lower for version 1.2. This is an effect of the difference in the predicted steam distribution within the LST vessel. There is less steam predicted in the near-wall node at elevation E (which corresponds to the bottom clime elevation) for version 1.2, resulting in a lower heat flux and a cooler film temperature at this elevation. At 10,000 seconds, the film exit temperatures for the two code versions for the second clime from the bottom are within 1.7°F.

The predicted air outlet temperature is shown in Figure 480.1023-11. The decrease in air outlet temperature when the fan comes on is apparent.

The predicted circumferentially averaged heat flux is shown as a function of height for test 214.1 phases A and B in Figures 480.1023-5 through 480.1023-7, respectively. As described above, the predicted heat flux is lower at elevation E (about 5 feet 6 inches from the vessel bottom) in version 1.2 due to the difference in the predicted steam distribution within the LST vessel.

LST 216.1

Test 216.1 has a constant steam flow and forced air cooling. The water was distributed over three quadrants for the first part of the test (216.1A) and over one quadrant for the second part of the test (216.1B).

The predicted heat rates into and out of the containment shell are shown in Figures 480.1023-14 and 480.1023-15, respectively. The downward spike is an effect of the instantaneous change in the code water coverage input value described in Reference 480.1023-1, Appendix B.

The predicted PCS film exit temperature is shown in Figure 480.1023-16. The predicted PCS air outlet temperature is shown in Figure 480.1023-17.

The predicted circumferentially averaged heat flux is shown as a function of height for test 216.1 phases A and B in Figures 480.1023-18 and 480.1023-19, respectively.

**LST 222.4**

Test 222.4 has a steam blowdown followed by a constant steam flow (222.4A). The steam flow rate was increased and allowed to come to a second steady state (222.4B). Steam was injected upward into the vessel through a 3-inch diameter nozzle located above the simulated operating deck. The non-condensable measurements showed this test has a more homogeneous concentration, including the lower deck region, relative to the tests discussed above. This has been attributed to the high kinetic energy from the smaller diameter nozzle. The measured water coverage for test 222.4 is described in Reference 480.1023-1, Appendix B.

The predicted heat rates into and out of the containment shell are shown in Figures 480.1023-20 and 480.1023-21, respectively. The downward spikes in heat rate are due to the instantaneous change in the code water coverage input value at 1500 seconds and 16,000 seconds.

The predicted PCS liquid film exit temperature and air outlet temperature are shown in Figures 480.1023-22 and 480.1023-23, respectively.

The predicted circumferentially averaged heat flux is shown as a function of height for test 222.4 steady state phases A and B in Figures 480.1023-24 and 480.1023-25, respectively.

References:

- 480.1023-1 WCAP-14967, "Assessment of Effects of WGOTHIC Solver Upgrade from Version 1.2 to 4.1," September 1997.
- 480.1023-2 WCAP-14382, "WGOTHIC Code Description and Validation," May 1995

SSAR Revision: NONE

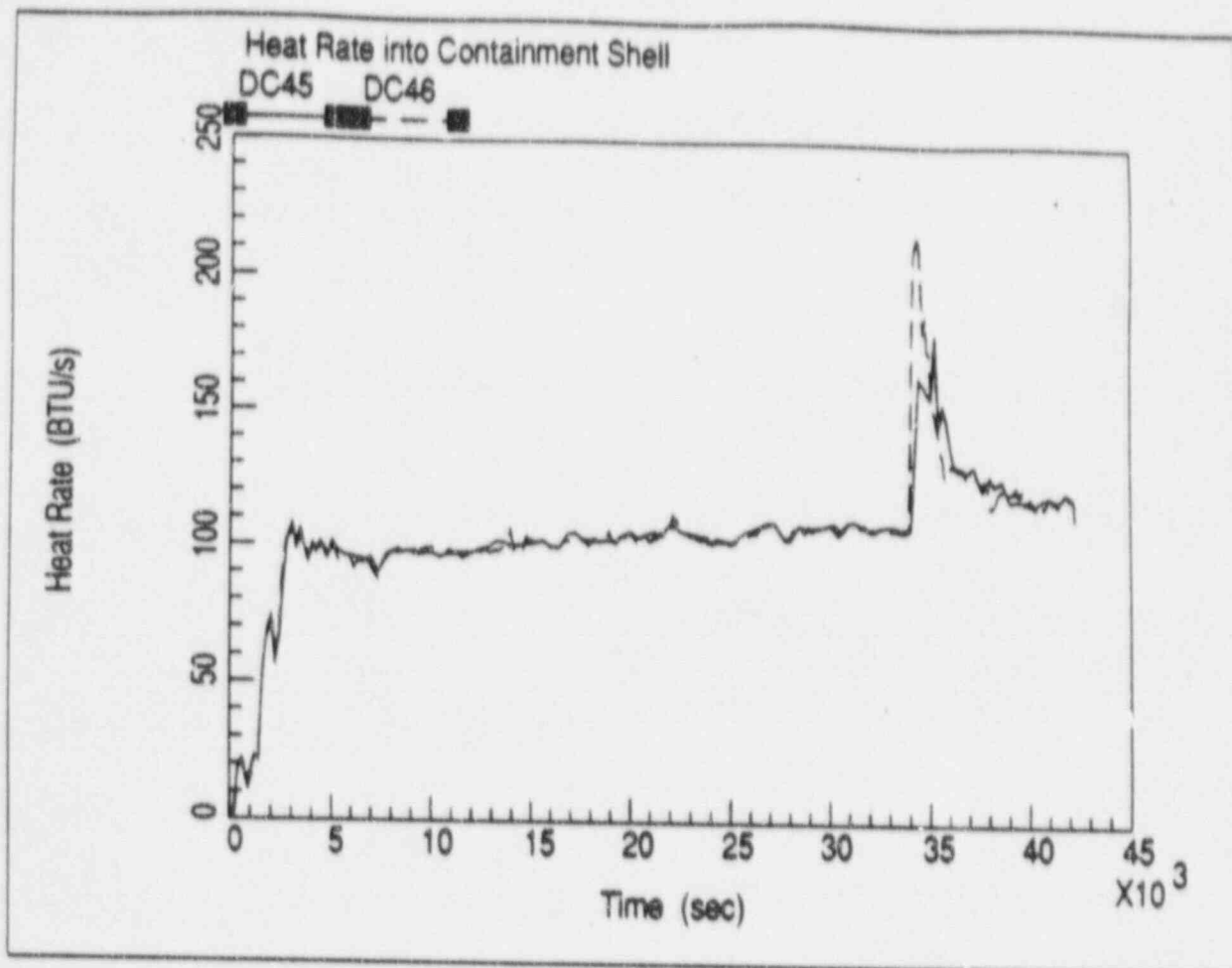


Figure 480.1023-1 Test 219.1 Heat Rate into Containment Shell

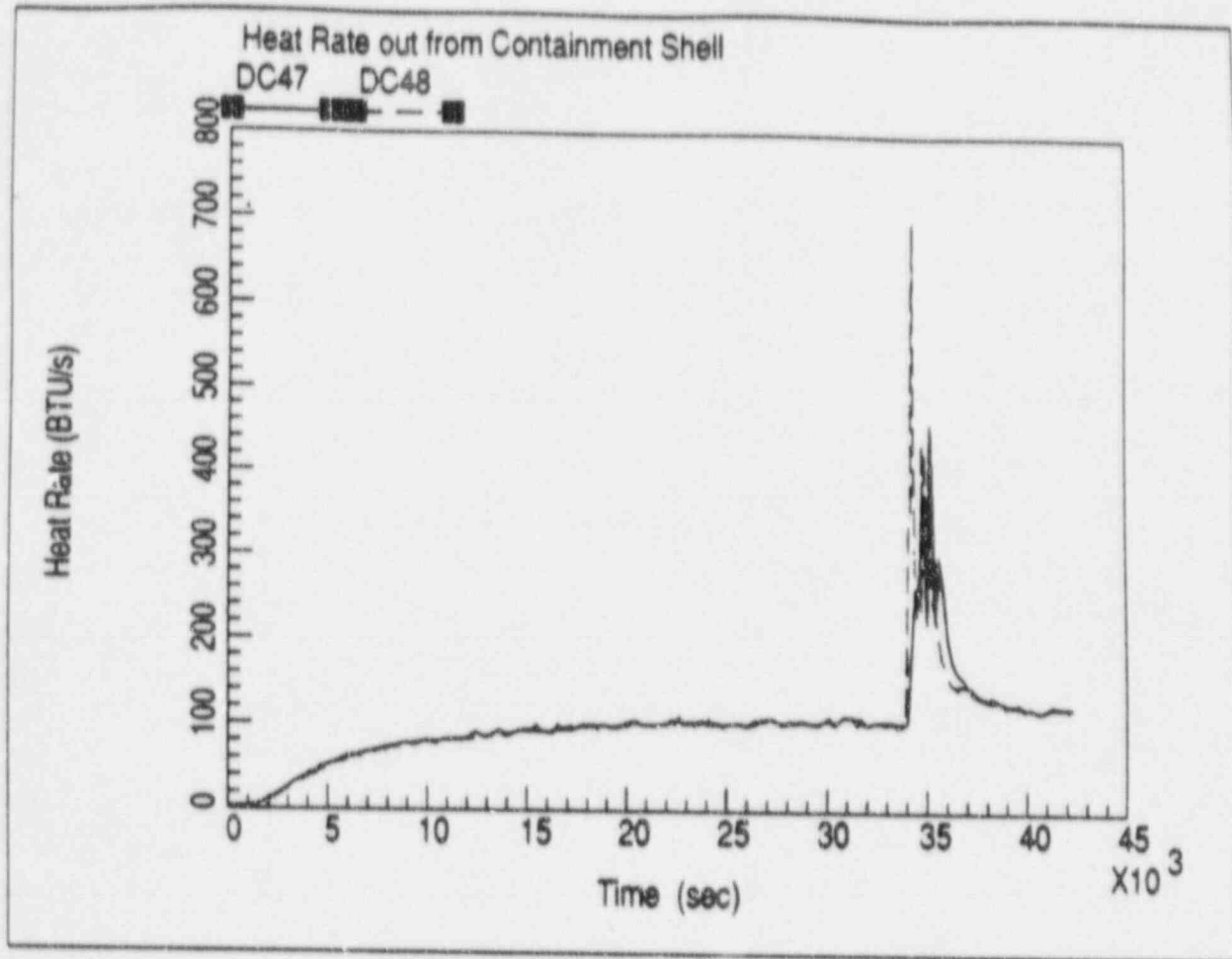


Figure 480.1023-2 Test 219.1 Heat Rate Out of Containment Shell

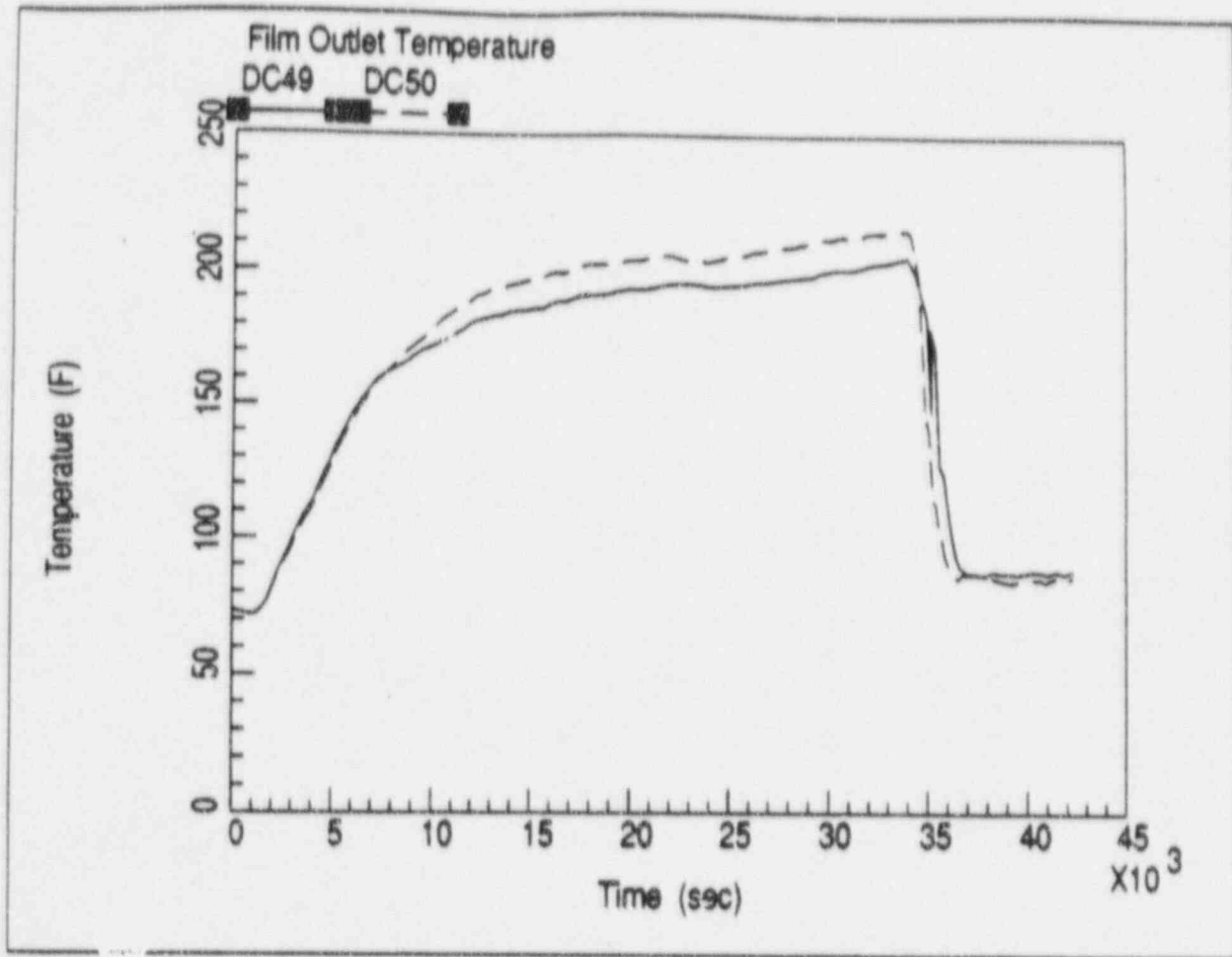


Figure 480.1023-3 Test 219.1 PCS Film Exit Temperature

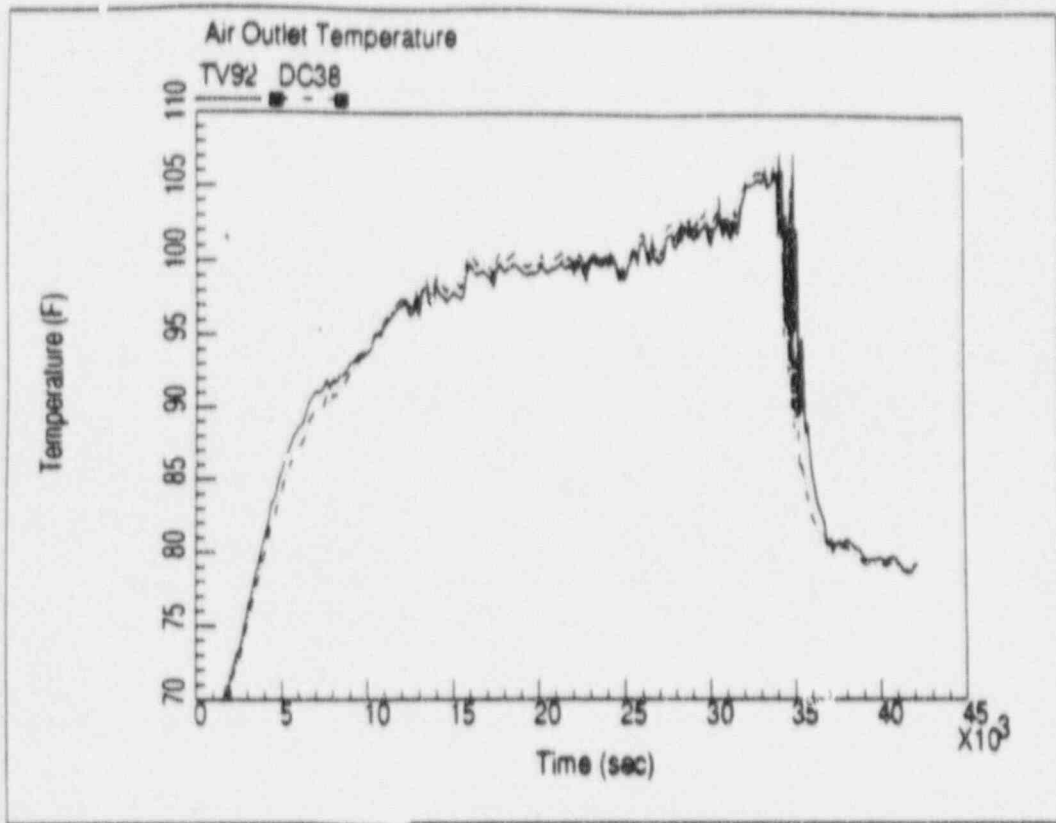


Figure 480.1023-4 Test 219.1 PCS Air Outlet Temperature

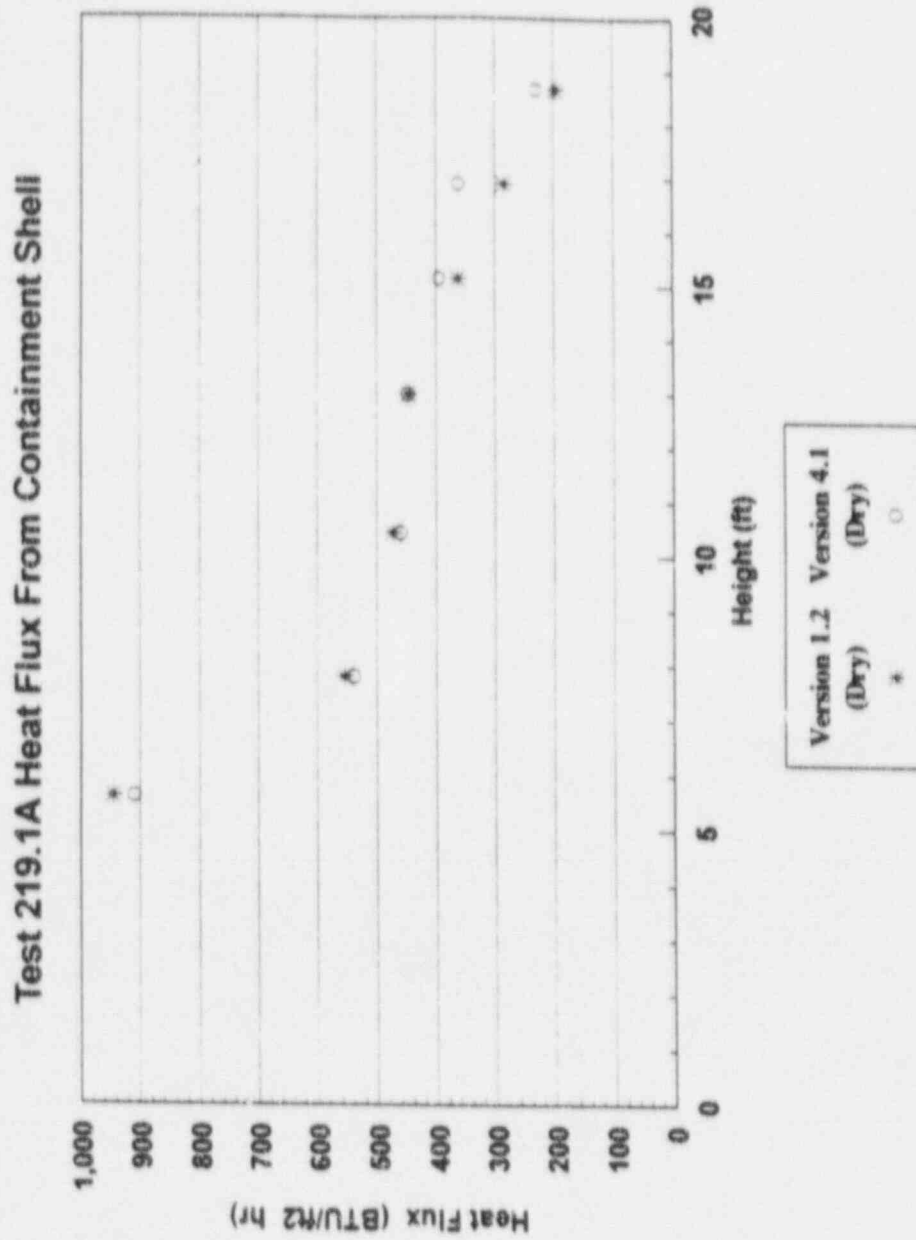


Figure 480.1023-5 Test 219.1 Steady-State Phase A Circumferentially Averaged Heat Flux vs. Height



Test 219.1B Heat Flux From Containment Shell

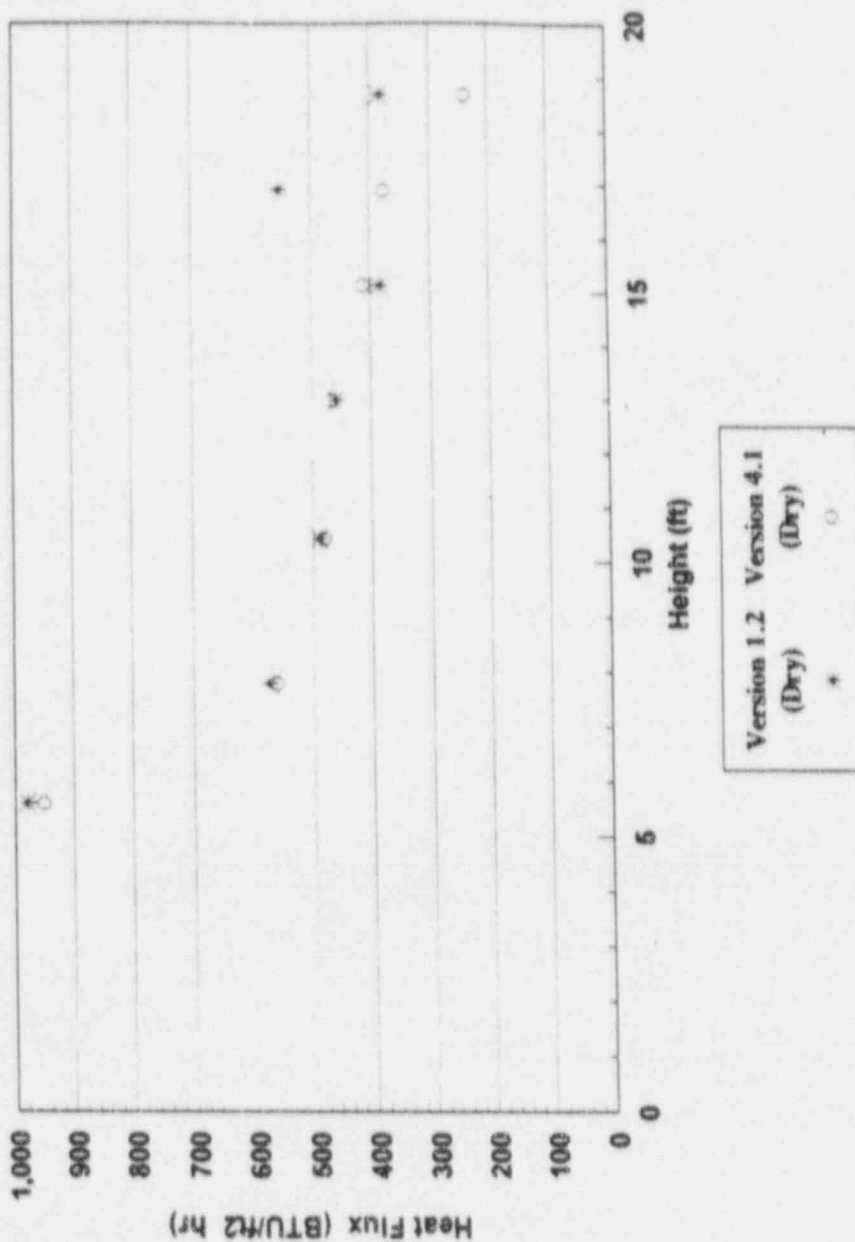


Figure 480.1023-6 Test 219.1 Steady-State Phase B Circumferentially Averaged Heat Flux vs. Height

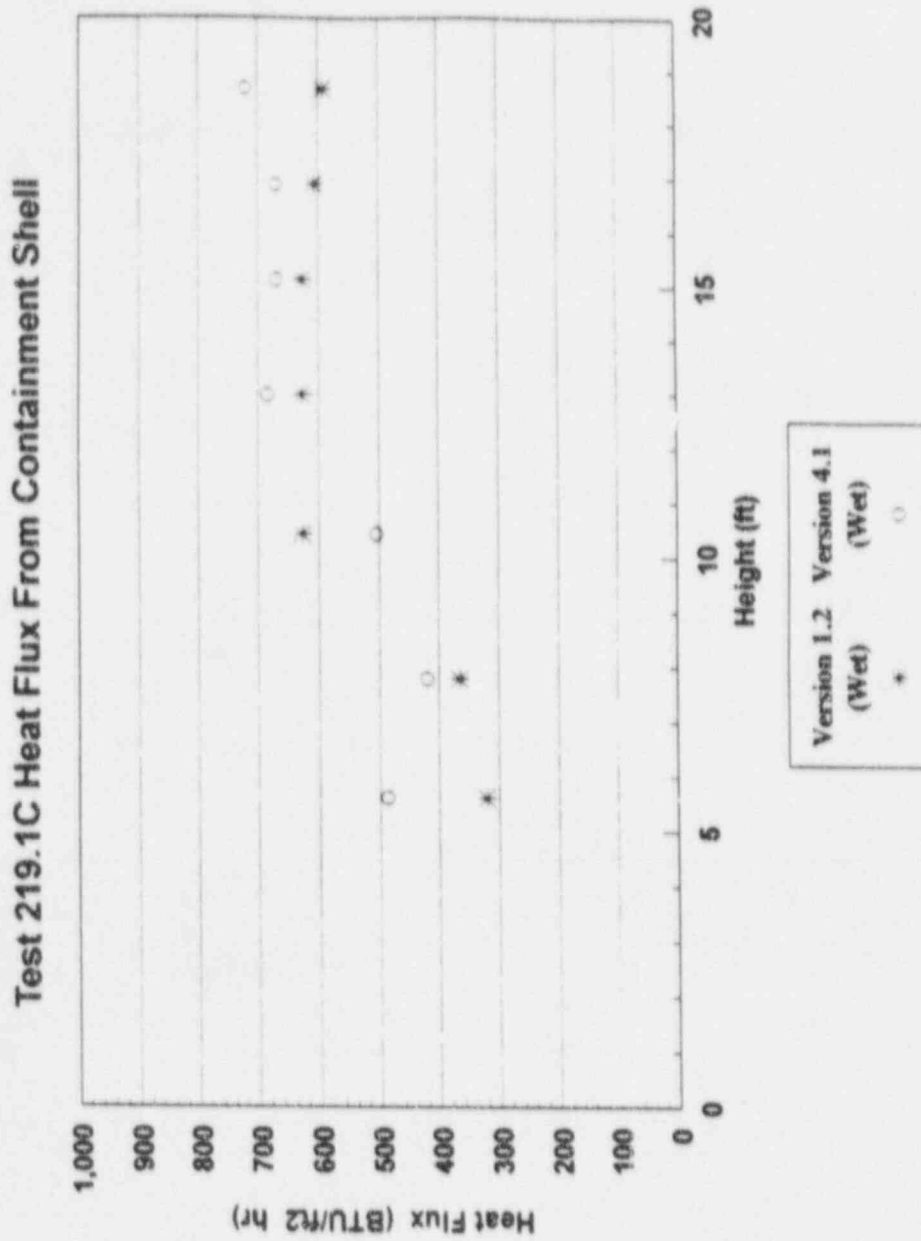


Figure 480.1023-7 Test 219.1 Steady-State Phase C Circumferentially Averaged Heat Flux vs. Height

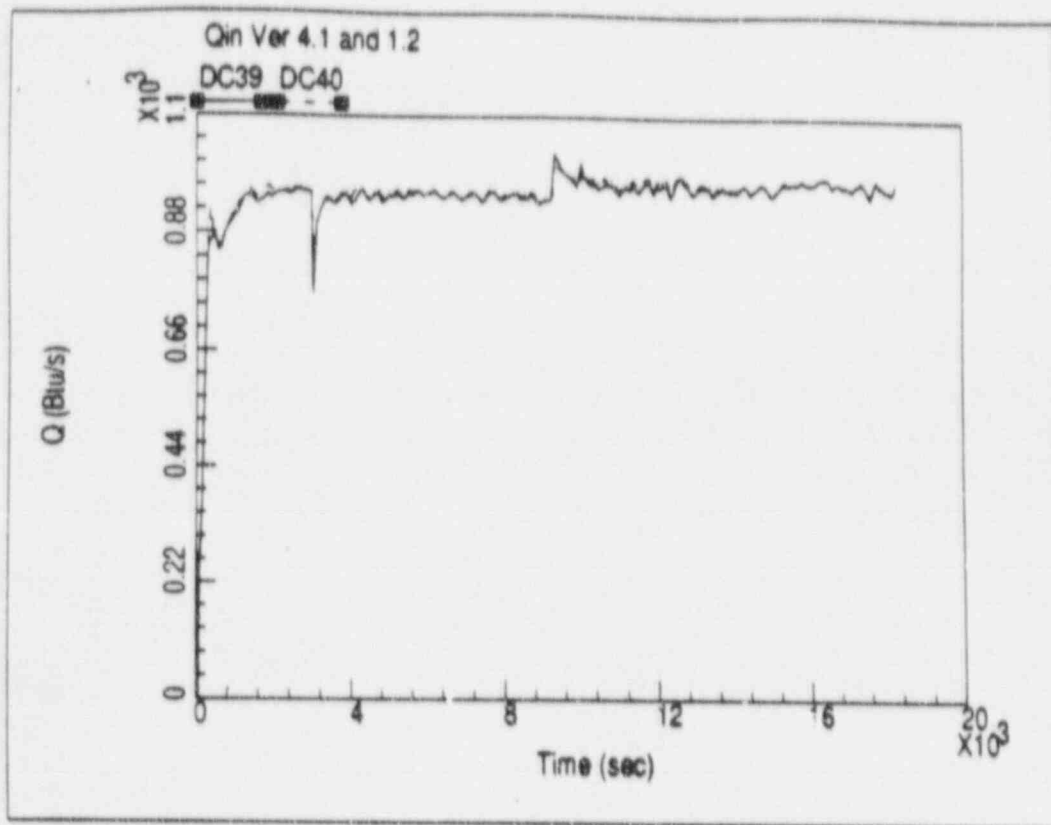


Figure 480.1023-8 Test 214.1 Heat Rate Into Containment Shell

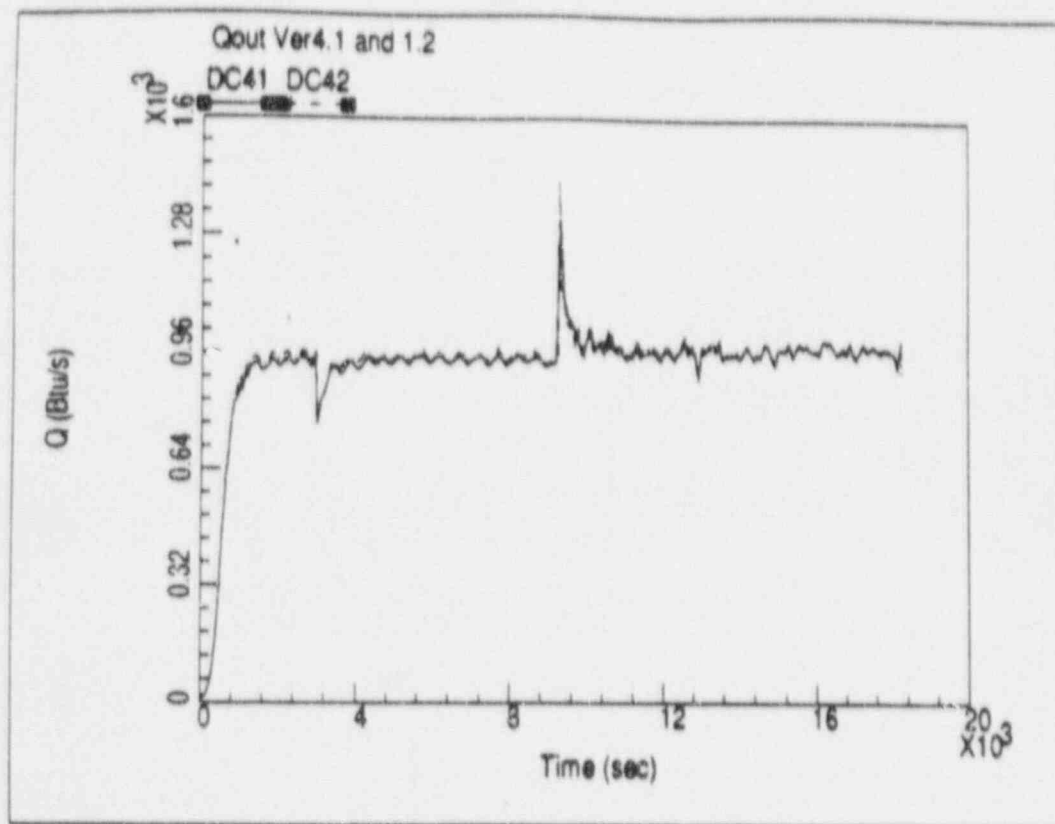


Figure 480.1023-9 Test 214.1 Heat Rate Out of Containment Shell

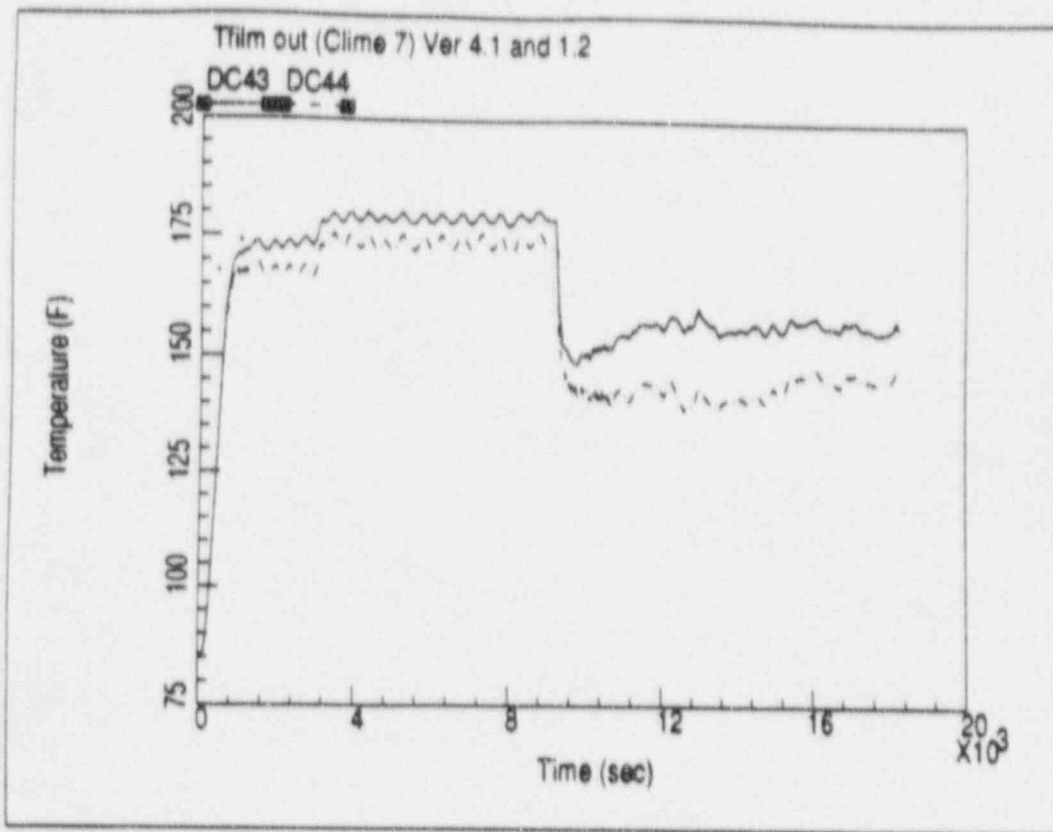


Figure 480.1023-10 Test 214.1 PCS Film Exit Temperature

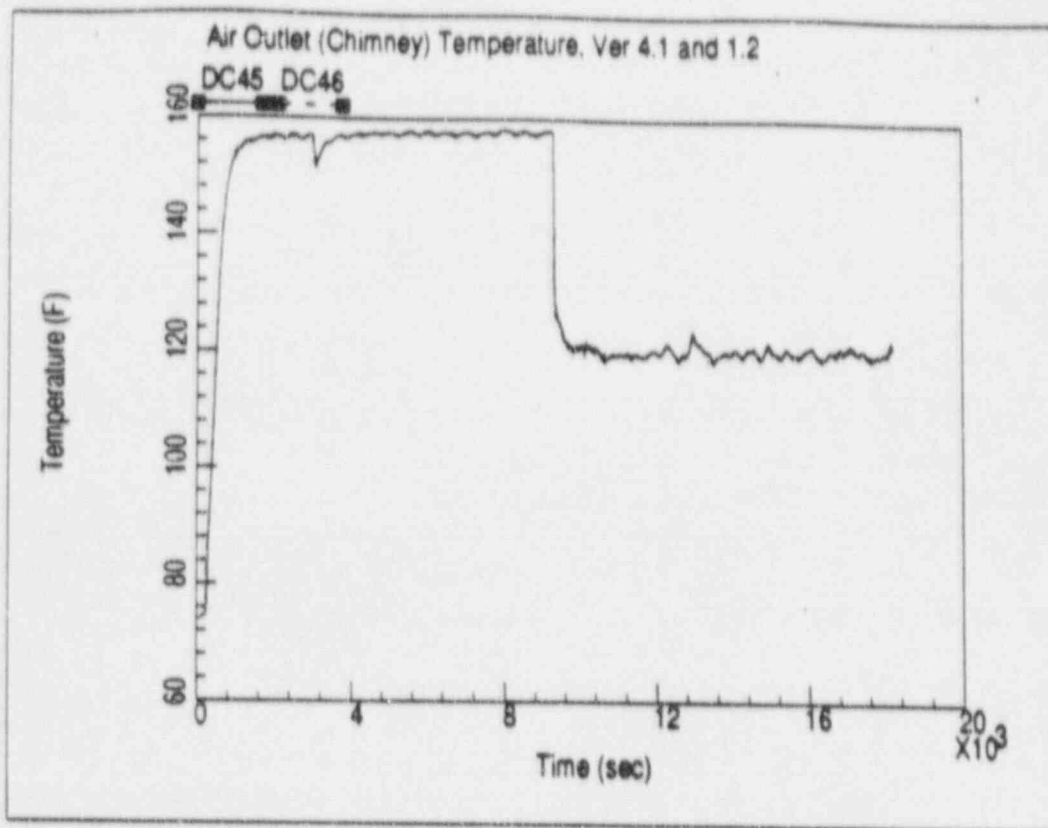


Figure 480.1023-11 Test 214.1 PCS Air Outlet Temperature

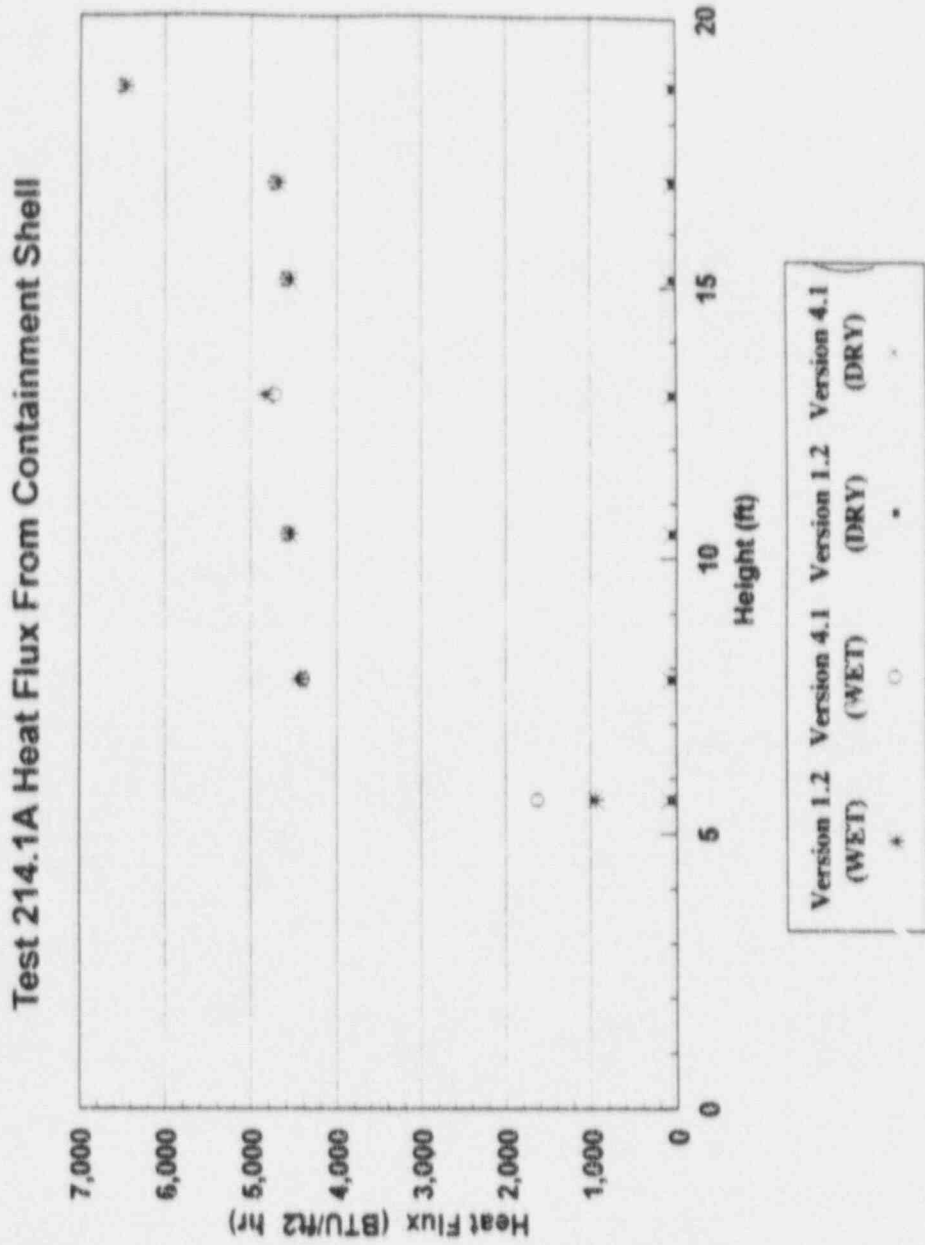


Figure 480.1023-12 Test 214.1 Steady-State Phase A Circumferentially Averaged Heat Flux vs. Height



Test 214.1B Heat Flux From Containment Shell

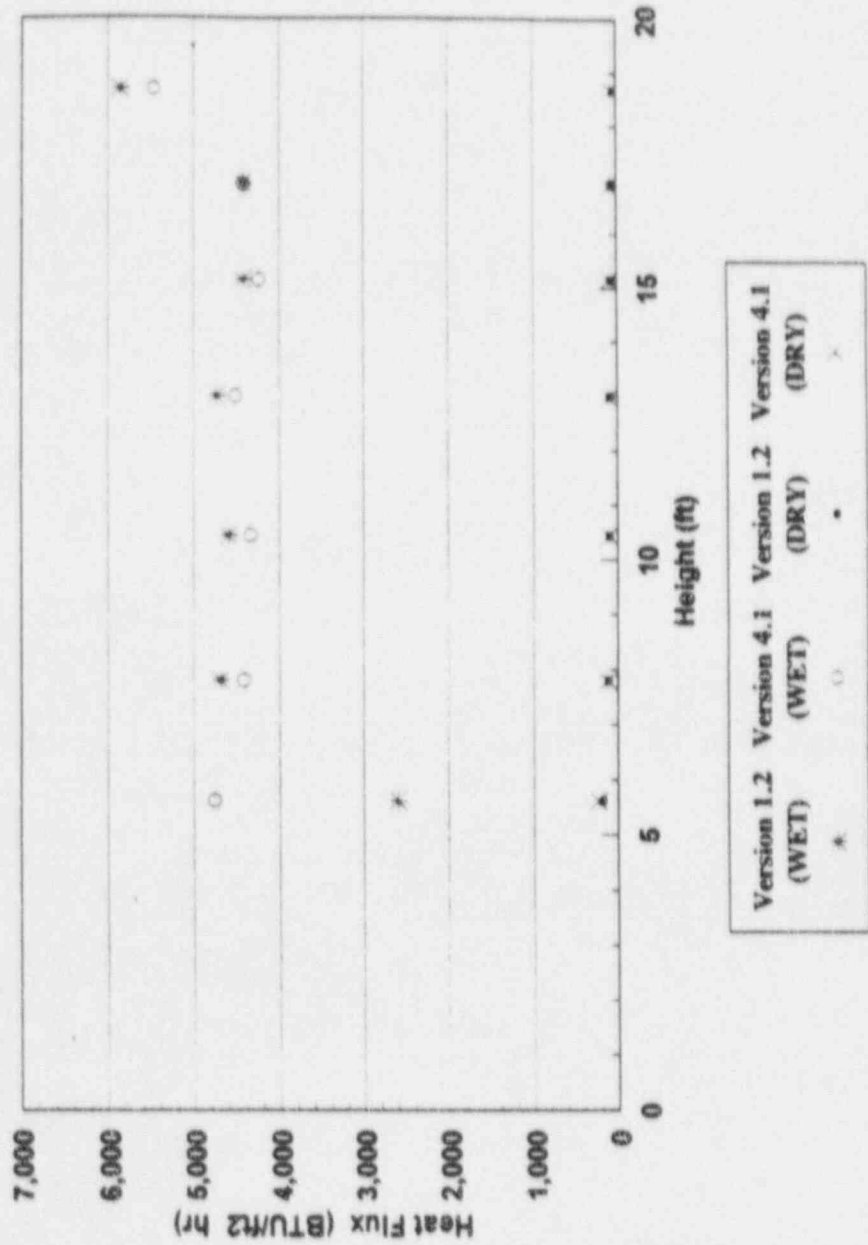


Figure 480.1023-13 Test 214.1 Steady-State Phase B Circumferentially Averaged Heat Flux vs. Height

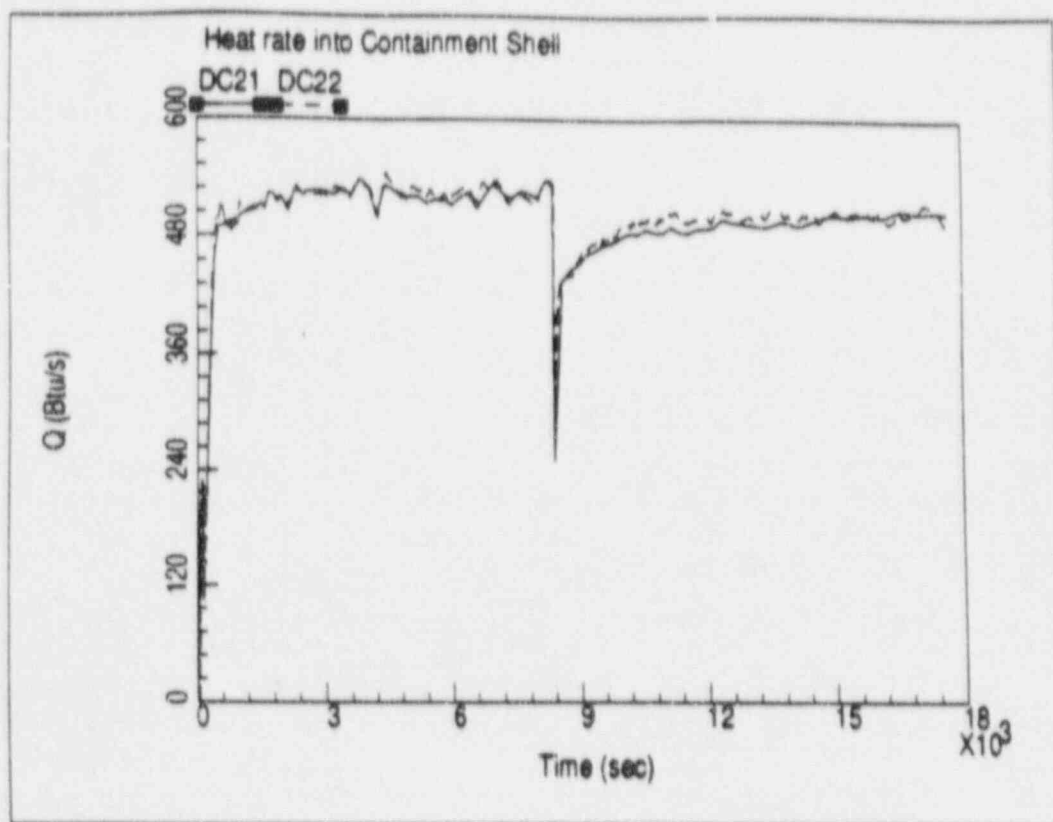


Figure 480.1023-14 Test 216.1 Heat Rate Into Containment Shell

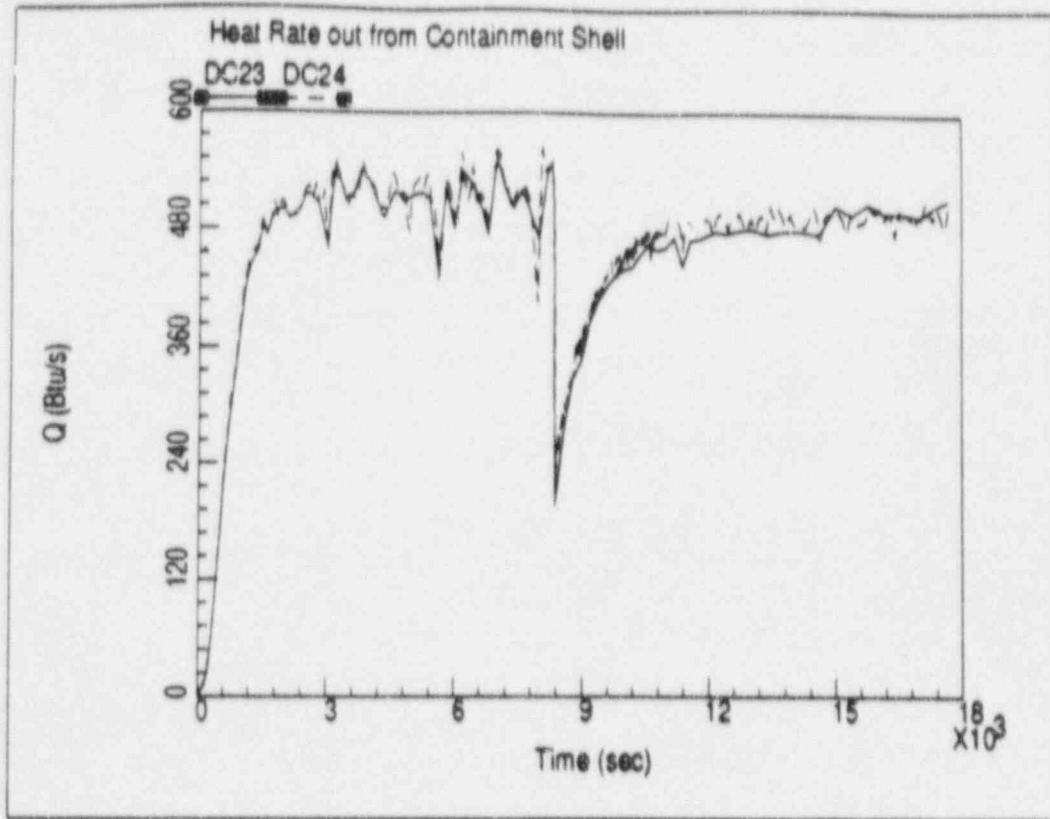


Figure 480.1023-15 Test 216.1 Heat Rate Out of Containment Shell

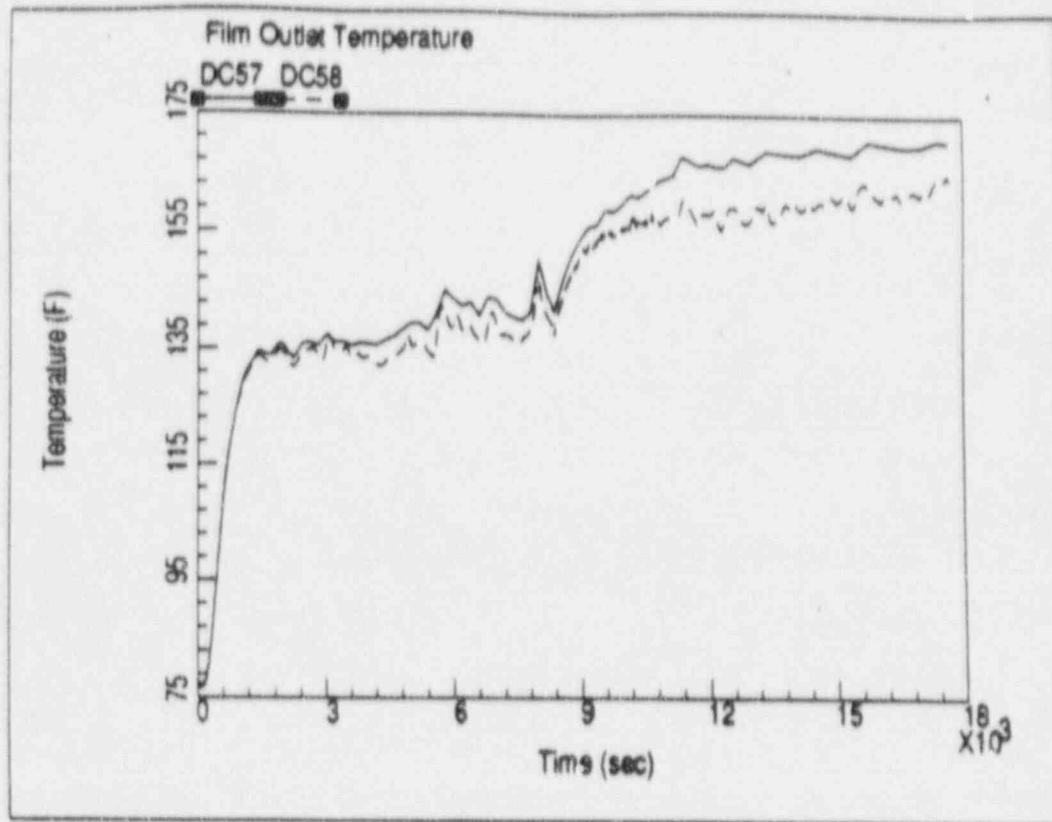


Figure 480.1023-16 Test 216.1 PCS Film Exit Temperature

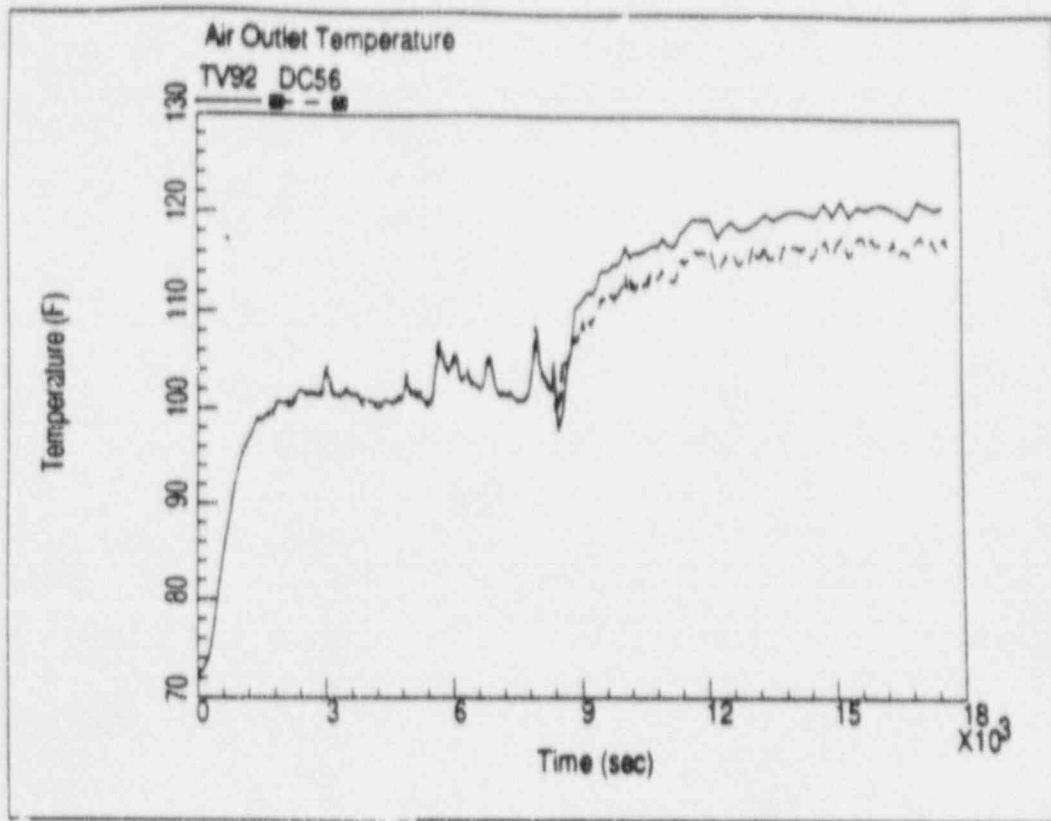


Figure 480.1023-17 Test 216.1 PCS Air Outlet Temperature

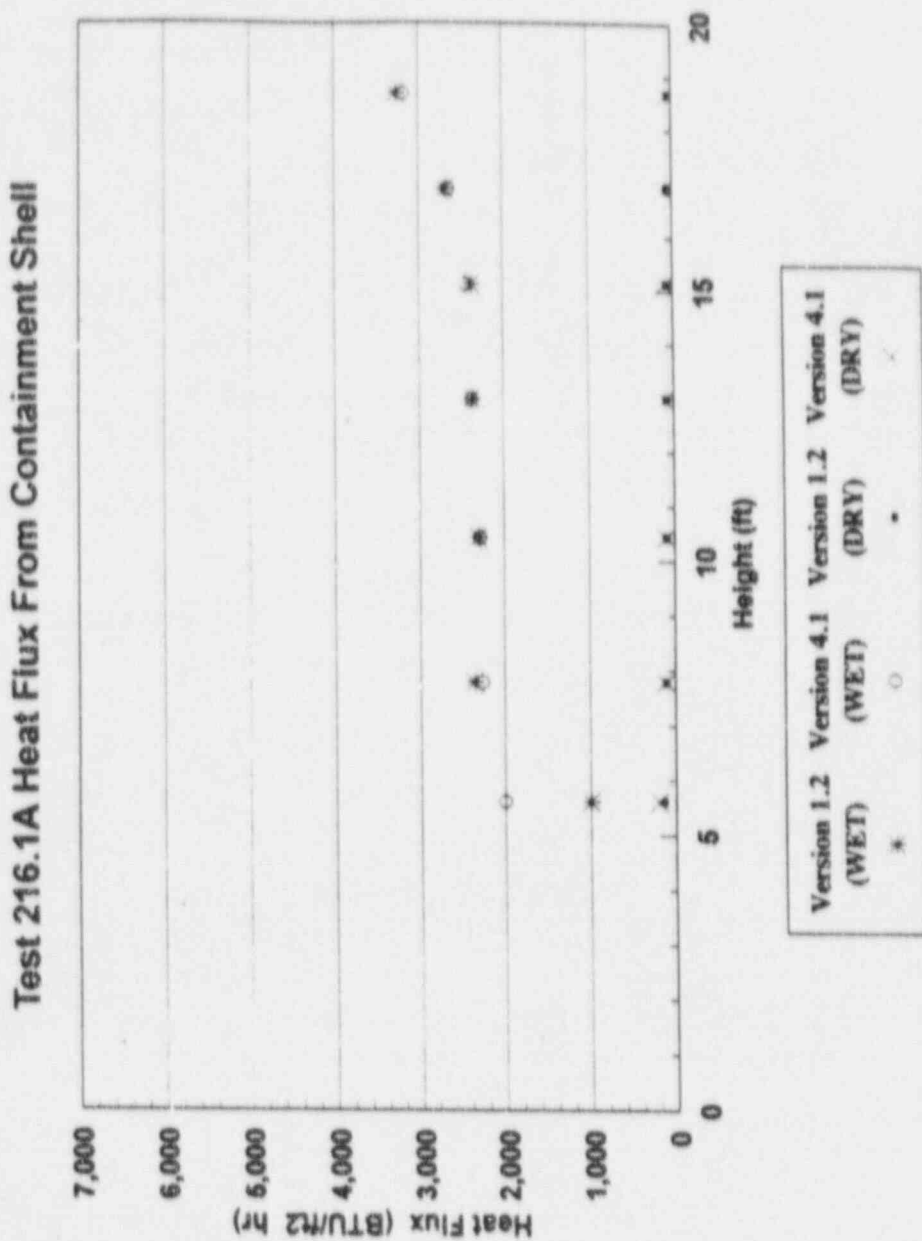


Figure 480.1023-18 Test 216.1 Steady-State Phase A Circumferentially Averaged Heat Flux vs. Height

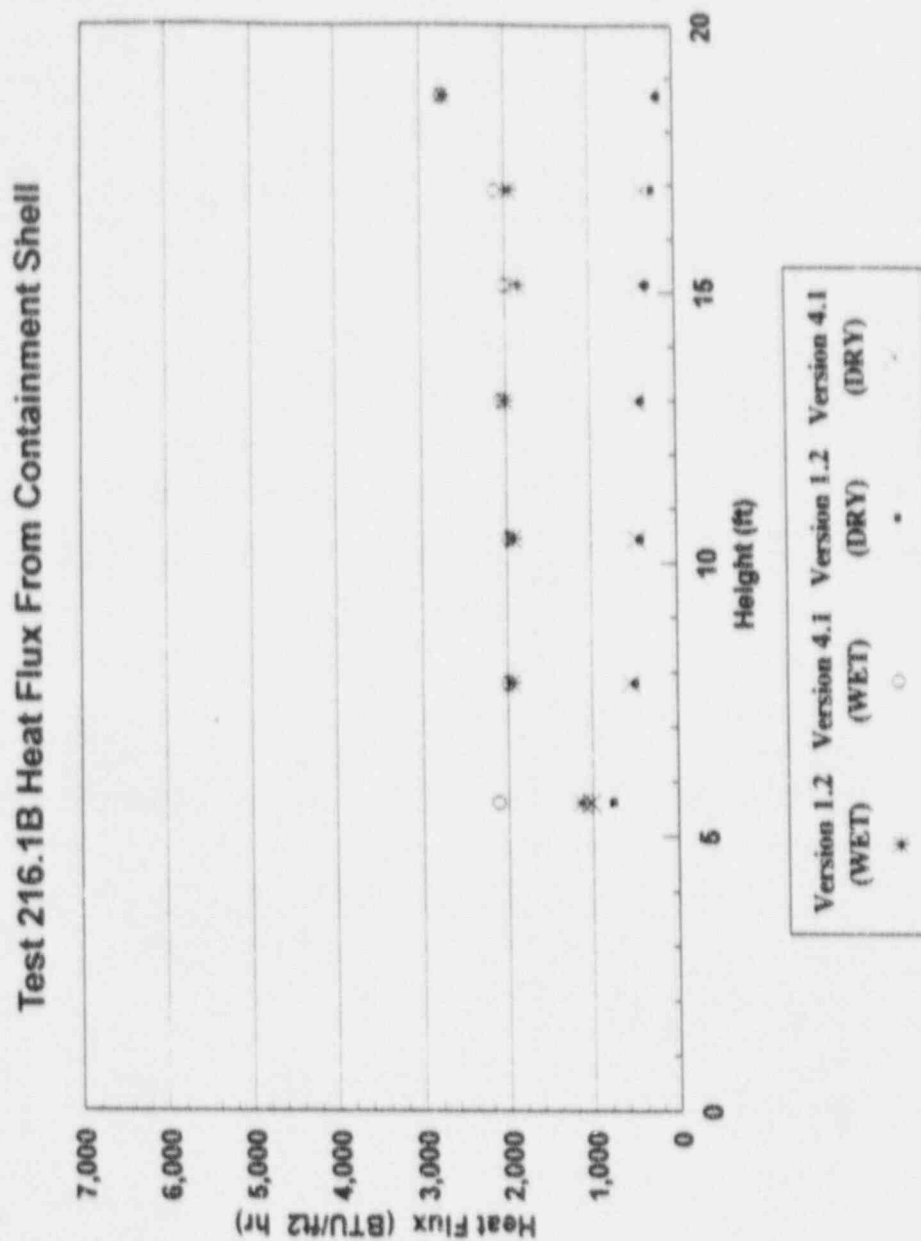


Figure 480.1023-19 Test 216.1 Steady-State Phase B Circumferentially Averaged Heat Flux vs. Height

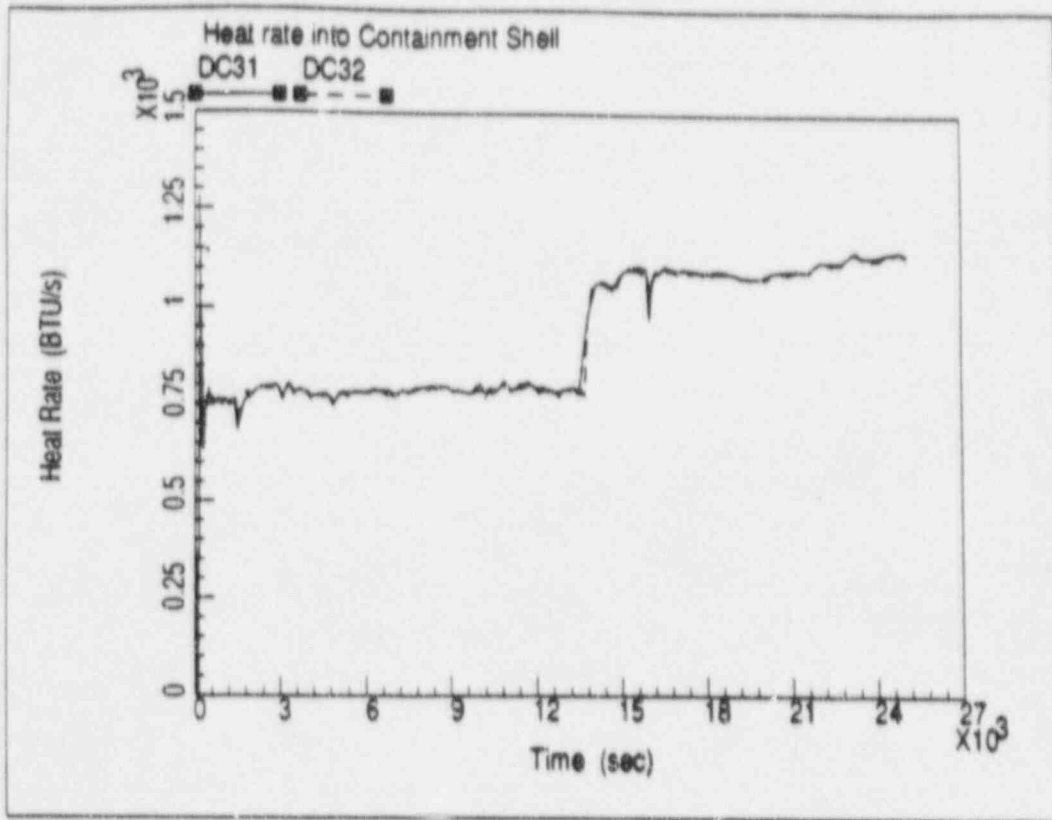


Figure 480.1023-20 Test 222.4 Heat Rate Into Containment Shell

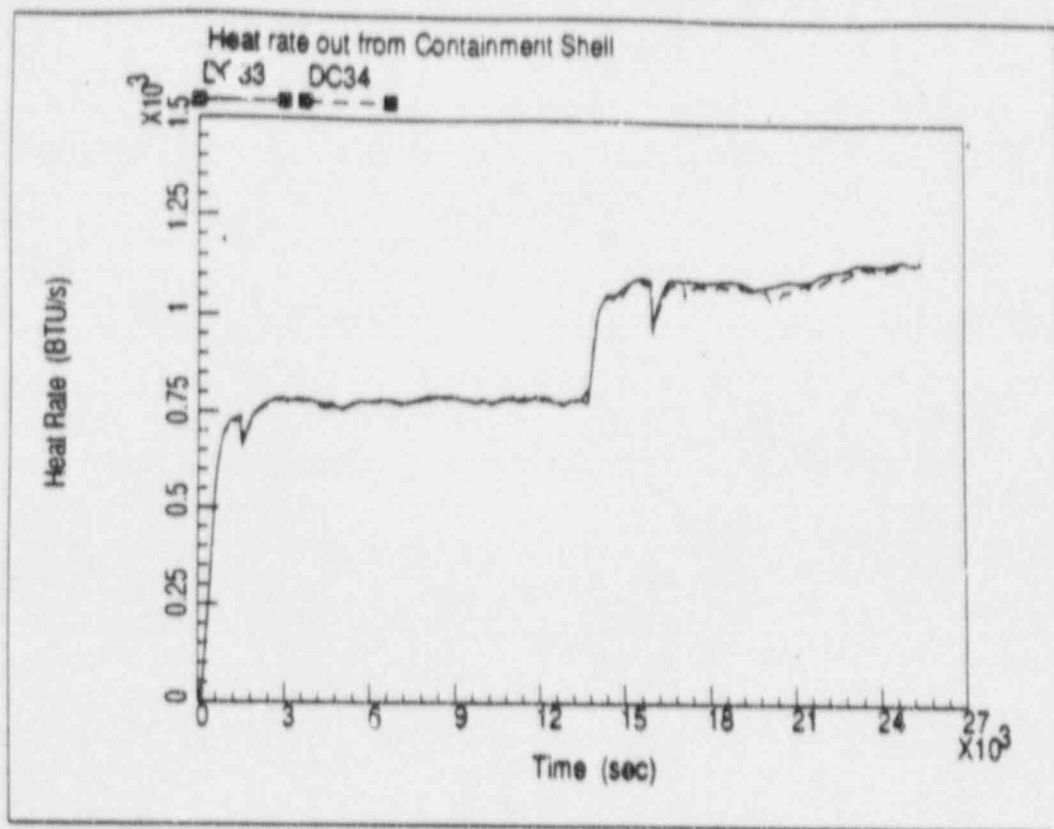


Figure 480.1023-21 Test 222.4 Heat Rate Out of Containment Shell

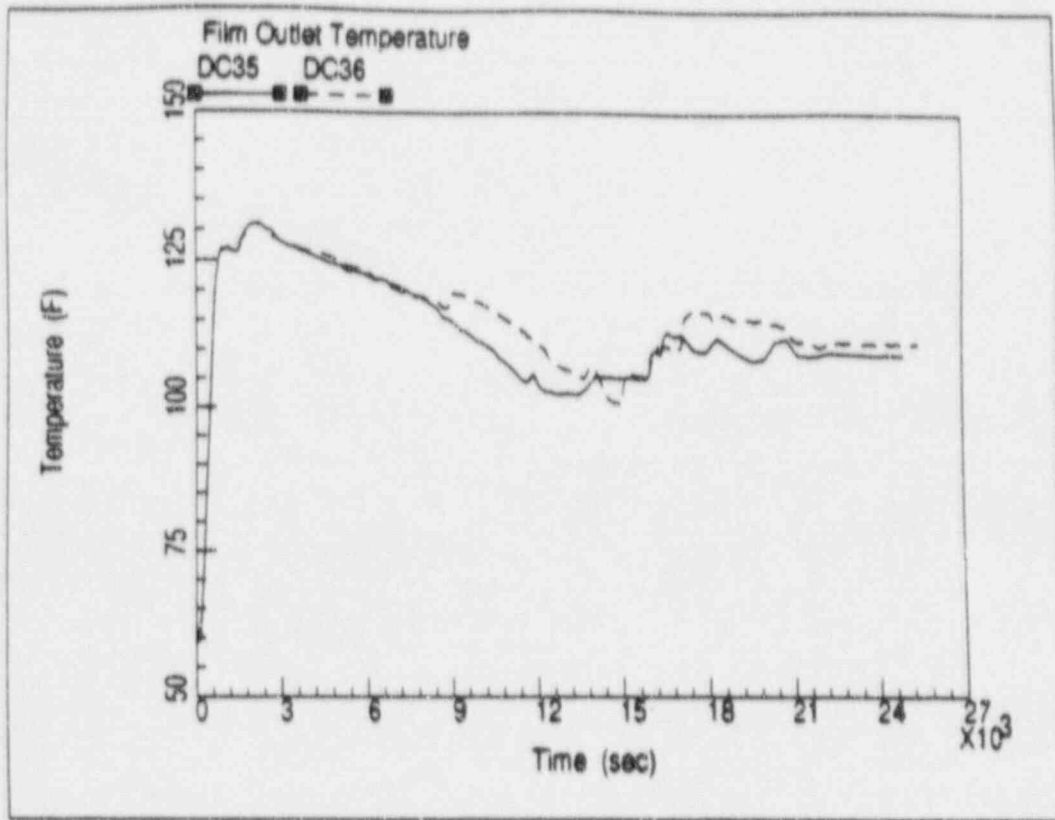


Figure 480.1023-22 Test 222.4 PCS Film Exit Temperature

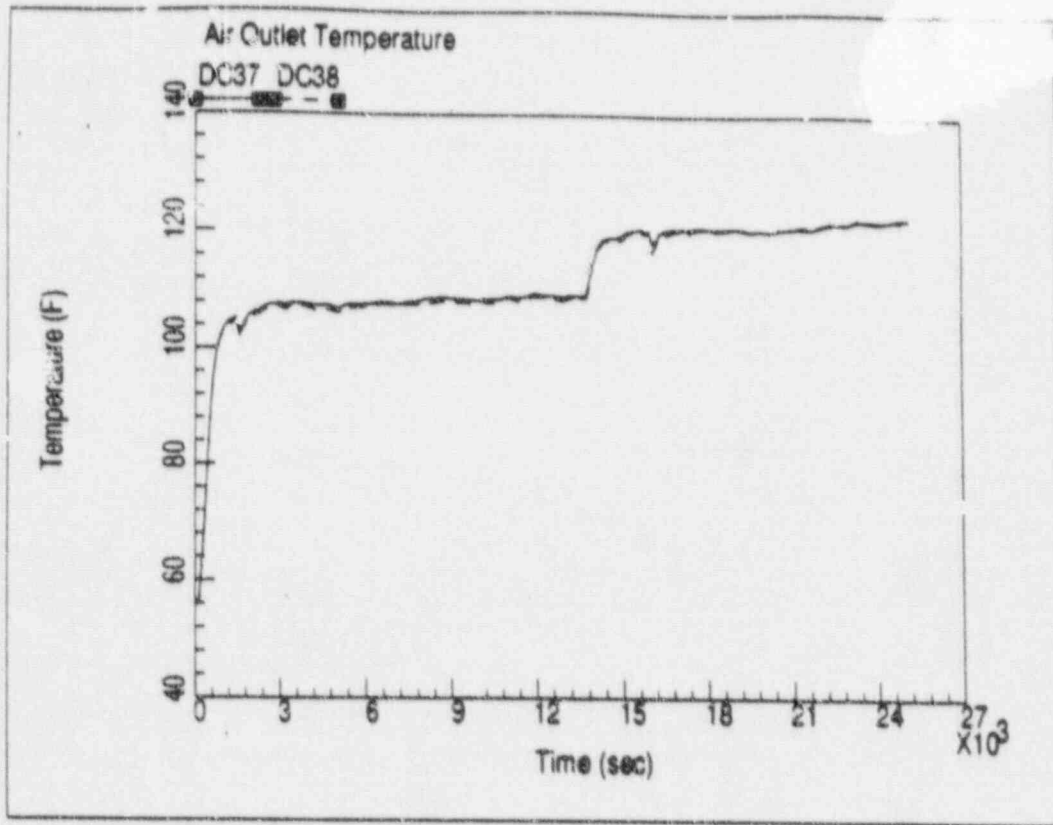


Figure 480.1023-23 Test 222.4 PCS Air Outlet Temperature

Test 222.4A Heat Flux From Containment Shell

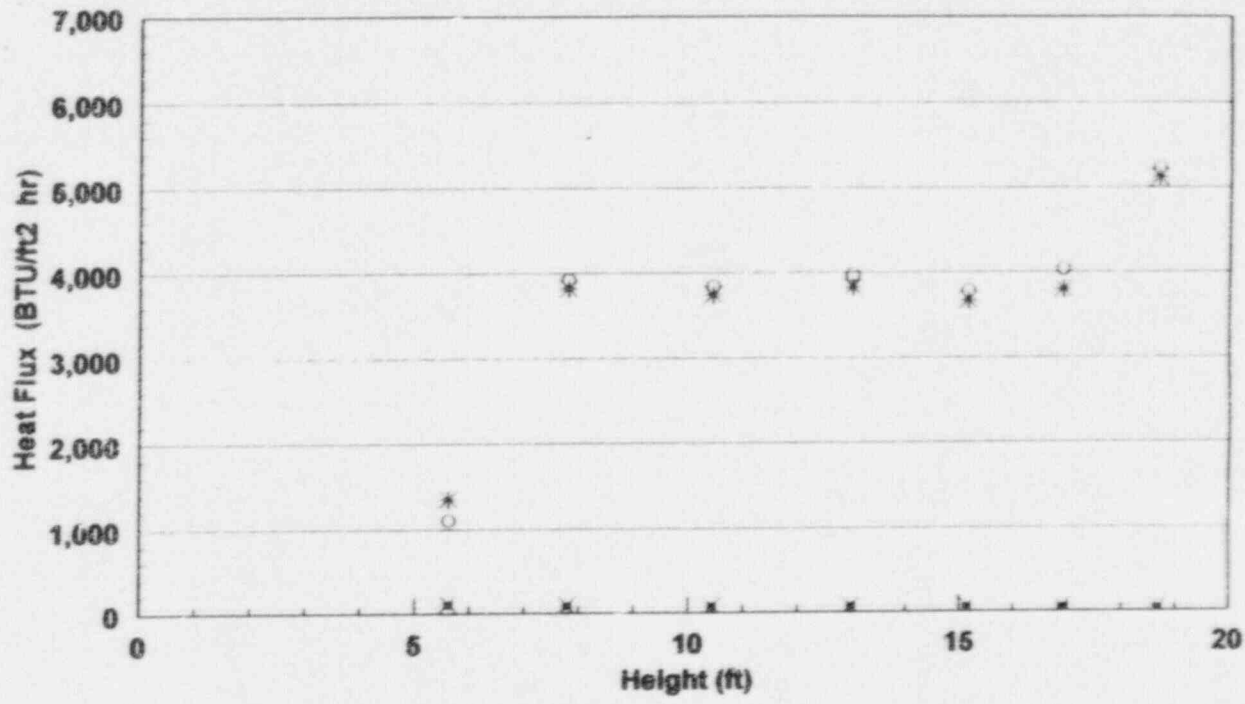


Figure 480.1023-24 Test 222.4 Steady-State Phase A Circumferentially Averaged Heat Flux vs. Height

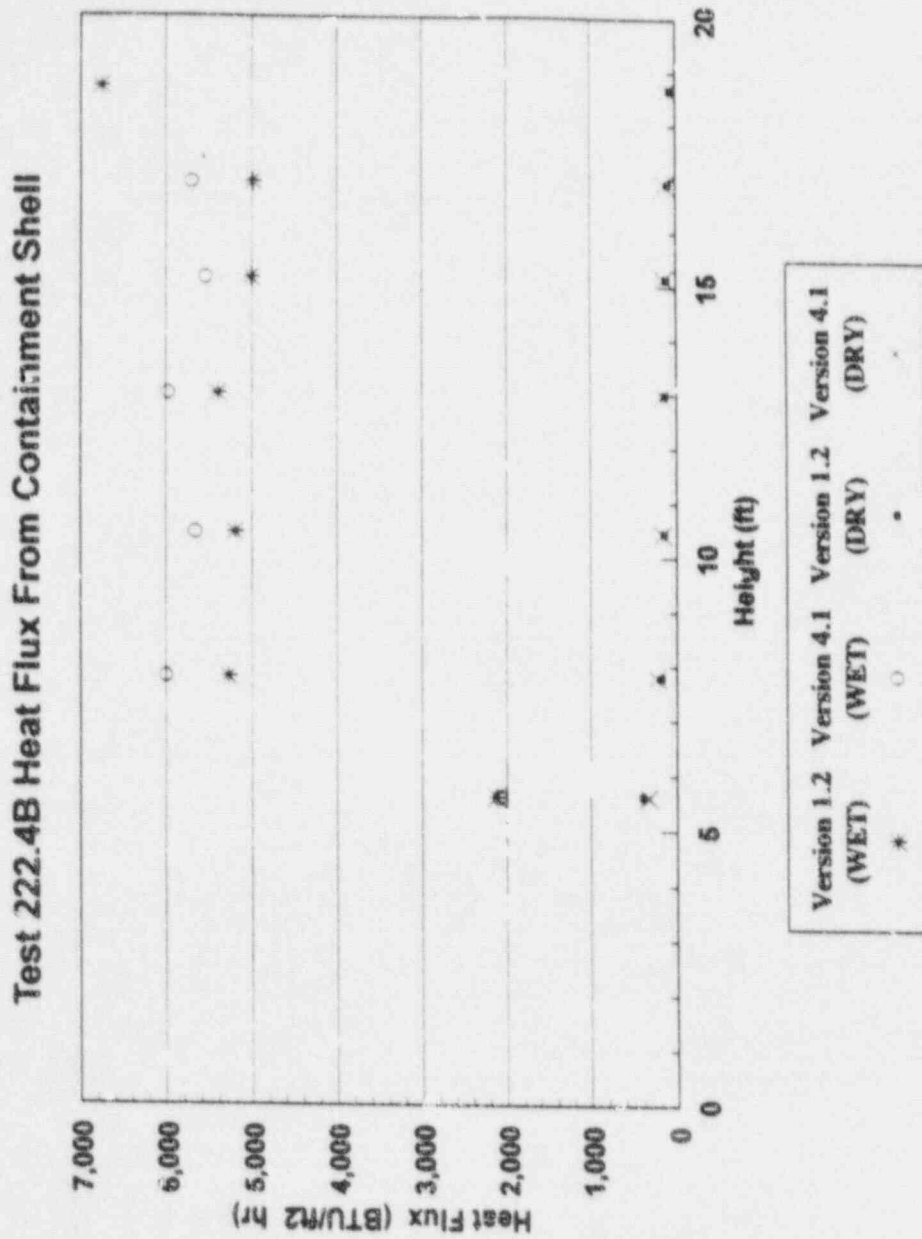


Figure 480.1023-25 Test 222.4 Steady-State Phase B Circumferentially Averaged Heat Flux vs. Height